ISET Journal of Earthquake Technology, Paper No. 522, Vol. 49, No. 3-4, Sept.-Dec. 2012, pp. 73–87

VARIABLE COEFFICIENT OF FRICTION: AN EFFECTIVE VFPI PARAMETER TO CONTROL NEAR-FAULT GROUND MOTIONS

Girish Malu* and Pranesh Murnal**

*Department of Civil Engineering
Dr. J.J. Magdum College of Engineering, Jaysingpur-416101
**Department of Applied Mechanics
Government College of Engineering, Aurangabad-431005

ABSTRACT

Several sliding isolation systems have been proposed to control earthquake effects. However, most of these isolation devices have limited effectiveness under the near-fault ground motions due to the pulse-type characteristics of such excitations. Recently proposed, VFPI has unique characteristics to overcome the limitations of a traditional isolation system for the near-fault ground motions. VFPI incorporates isolation, energy dissipation and restoring force mechanisms and has additional advantages due to the response-dependent variable frequency of oscillation and bounded restoring force. The device has wide choice of parameters to choose from, as per the design requirements. In this paper, the behaviour of single-storey structures isolated by using VFPI and subjected to the near-fault ground motions is numerically examined. It is shown that it is possible to increase the effectiveness of VFPI by using a discretely-varying coefficient of friction along the sliding surface. Parametric studies are carried out to critically examine the behaviour of single-storey structures isolated with the VFPI and FPS systems.

KEYWORDS: Base Isolation, VFPI, Near-Fault Ground Motions, Passive Control

INTRODUCTION

Base isolation has emerged as an effective technique in minimizing the earthquake forces. In this technique, a flexible layer (or isolator) is placed between the super-structure and its foundation such that relative deformations are permitted at this level. Due to the flexibility of the isolator layer, the time period of the motion of the isolator is relatively long; as a result, the isolator time period controls the fundamental period of the isolated structure. For a properly designed isolation system, the isolator time period is much longer than the periods containing significant ground-motion energy. As a result, the use of isolator shifts the fundamental period of the structure away from the predominant periods of ground excitation. An extensive review of the base-isolation systems and their applicability is available in literature (Buckle and Mayes, 1990; Kelly, 1993; Naeim and Kelly, 1999).

The practical isolation devices typically include an energy dissipating mechanism also, so as to reduce the deformations at the isolator level. For example, the friction-type base isolators use a sliding surface for both isolation and energy dissipation and have been found to be very effective in reducing the structural response (Mostaghel et al., 1983). Due to the characteristics of the excitation transmitted through the sliding surface, the performance of friction isolators is relatively insensitive to the severe variations in the frequency content and amplitude of the input excitation, thus making the performance of sliding isolators very robust. The simplest sliding isolator consists of a horizontal sliding surface (in the pure friction or PF system), which may experience large sliding and residual displacements. It is therefore often difficult to incorporate such an isolator in structural design.

In order to overcome the difficulty with providing restoring force, an effective mechanism to provide restoring force by gravity has been utilized in the friction pendulum systems (FPSs) (Zayas et al., 1987). In this system, the sliding surface takes a concave spherical shape so that the sliding and re-centering mechanisms are integrated into one unit. The FPS isolator has several advantages over the PF system and has demonstrated acceptable performance for many different structures and excitation characteristics (Mokha et al., 1990; Tsopelas et al., 1996; Tsai, 1997; Wang et al., 1998). However, the main disadvantage of a FPS is that it has a constant time period of oscillation due to its spherical surface. As a result, the FPS isolators can be effectively designed for a specific level (of amplitude and frequency characteristics) of the ground excitation. Under more severe ground motions, sliding displacements

greater than the design displacement can occur, which may lead to very large accelerations and thus to the failure of FPS isolator. Since in a FPS isolator, the restoring force is linearly proportional to the sliding displacement, the large amount of sliding introduces significant additional energy in the structure. As a result, the maximum intensity of excitation has a strong influence on the FPS design. In general, a FPS isolator designed for a particular level of excitation may not give satisfactory performance during an earthquake with much lower or higher intensity (Sinha and Pranesh, 1998). Due to the constant value of frequency, a resonant problem may occur when the structure resting on a FPS is subjected to a ground motion of dominant frequency close to the isolation frequency (Krishnamoorthy, 2010).

Due to the limitations of FPS, many researchers have tried different geometries for the sliding surface of the isolator. A recently developed new isolator, called as the variable frequency pendulum isolator (VFPI), incorporates the advantages of both FPS and PF isolators and overrules the disadvantages of FPS and PF isolators (Pranesh and Sinha, 1998; Pranesh, 2000). This is probably the first attempt to propose the concept of variable frequency in the sliding type isolators, although the concept of variable curvature is found in literature earlier (Sustov, 1992). Lu et al. (2006) generalized the mathematical formulation of a sliding surface with variable curvature by using a polynomial function to define the geometry of the sliding surface. In this paper an experimental and analytical study of the performance of three sliding-type isolators (including VFPI) is carried out. Krishnamoorthy (2010) also proposed a sliding surface with variable frequency and friction coefficient. This study proposed an isolator having the radius of curvature varying exponentially with sliding displacement and friction coefficient also varying with the sliding displacement. However, VFPI is found to be more effective under a variety of excitations and structures because of the following properties of VFPI: (1) its time period of oscillation depends on the sliding displacement, and (2) its restoring force has a bounded value and exhibits softening behaviour for the large displacements (Malu and Murnal, 2010). The geometry of sliding surface is defined by a second-order parametric equation. As a result, the isolator properties can be chosen to achieve the progressive period shift with a variation in the sliding displacement. These properties can be controlled by a set of VFPI parameters, which is otherwise not possible in the single-parameter systems like FPS.

The study of structures subjected to near-fault ground motions has a special significance due to the nature of such ground motions. The near-fault ground motions are characterized by pulse-type excitations having a narrow range of relatively lower frequencies. These motions often contain strong coherent dynamic long-period pulses and permanent ground displacements. The dynamic motions are dominated by the large long-period pulses of motions that are caused by the rupture directivity effects and occur on the horizontal component perpendicular to the strike of fault. This pulse is a narrow-band pulse which causes the response spectrum to have a peak, such that the response due to the near-fault ground motions of moderate magnitudes may exceed the response due to the near-fault ground motions of large magnitudes at intermediate periods. The radiation pattern of the shear dislocation on the fault causes this large pulse of motion to be oriented in the direction perpendicular to the fault plane, thus causing the strike-normal component of the ground motion to be larger than the strike-parallel component. The strike-parallel motion causes a permanent ground displacement (i.e., fling step), whereas the strike-normal component causes a significantly higher dynamic motion (Somerville, 1997, 2005).

The structures isolated by most base isolation devices have long time periods which are fairly constant. Since the near-fault ground motions are long-period, pulse-type motions, those induce very large displacements at the isolation level. As a result, base-isolated structures do not perform well under the near-fault ground motions. However, it has been demonstrated that the newly developed isolator VFPI can be effective under both near-fault and far-field ground motions, if proper VFPI parameters are adopted in the design (Murnal and Malu, 2007; Malu and Murnal, 2010). However, it is difficult to control the large sliding displacements that could occur during the near-fault ground motions.

In the present paper, it is proposed to change the coefficient of friction at a predefined location along the VFPI isolator surface so that the sliding displacement can be controlled under the near-field ground motions. A smaller value of the coefficient of friction for smaller sliding displacements and a larger value for larger sliding displacements is likely to control the displacement due to the higher energy dissipation due to the increased friction force. The effectiveness of a VFPI with discretely variable coefficient of friction is examined through a parametric study on the single-degree-of-freedom (SDOF) models (i.e., 2-DOF models when isolated) subjected to near-fault ground motions.

VFPI DESCRIPTION

1. Mathematical Preliminaries

Consider the motion of a rigid block of mass m sliding on a smooth curved surface of the defined geometry, $y = f(x)$. The restoring force offered by the curved sliding surface can be defined as the lateral force required to cause the horizontal displacement x. Assuming a point contact between the block and the sliding surface, various forces acting on the sliding surface, when the block is displaced from its original position at the origin of coordinate axes, are as shown in Figure 1. At any instant, the horizontal restoring force due to the weight of the structure is given by

$$f_R = mg\frac{\mathrm{d}y}{\mathrm{d}x} \tag{1}$$

Assuming that the restoring force is mathematically represented by an equivalent nonlinear massless horizontal spring, the spring force can be expressed as the product of the equivalent spring stiffness and deformation, i.e.,

$$f_R = k(x)x \tag{2}$$

where $k(x)$ is the instantaneous spring stiffness, and x is the sliding displacement of the mass.

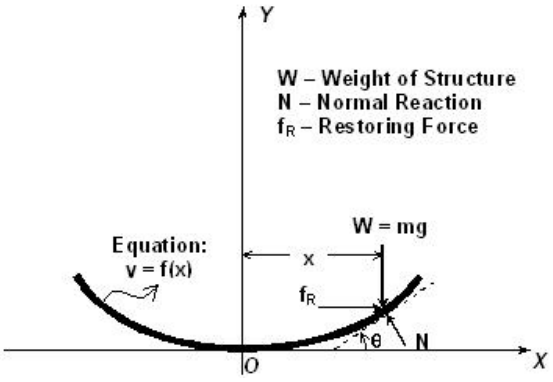

Fig. 1 Free-body diagram of sliding surface

If the mass is modelled as a single-degree-of-freedom oscillator, the spring force (or restoring force) can be expressed as the product of the total mass of the system and square of oscillation frequency:

$$f_R = m\omega_b^2(x)x \tag{3}$$

Here, $\omega_b(x)$ is the instantaneous isolator frequency; this depends solely on the geometry of the sliding surface. In a friction pendulum system, which has a spherical sliding surface, this frequency is almost constant and is approximately equal to $\sqrt{g/R}$, where R is the radius of curvature of the sliding surface (Zayas et al., 1990).

2. Variable Frequency Pendulum Isolator Geometry

A sliding surface based on the expression of an ellipse has been used as the basis for developing the sliding surface of VFPI (Pranesh, 2000). The equation of an ellipse with a and b as its semi-major and semi-minor axes, respectively, and with the coordinate axes as shown in Figure 1 is given by

$$y = b\left(1-\sqrt{1-x^2/a^2}\right) \tag{4}$$

On differentiating with respect to x, the slope at any point on the curve is given by

$$\frac{\mathrm{d}y}{\mathrm{d}x} = \frac{b}{a^2\sqrt{1-x^2/a^2}}x \tag{5}$$

If the equation of sliding surface is represented by Equation (4), the frequency of oscillation can be determined by substituting Equation (5) in Equations (1) and (3). As a result, the expression for the frequency of elliptical surface is given by

$$\omega_b^2(x) = \omega_I^2 \Big/ \sqrt{1 - x^2/a^2} \tag{6}$$

where $\omega_I^2 = gb/a^2$ is the square of the initial frequency of the isolator (at the zero sliding displacement).

It can be seen that the frequency of an elliptical curve is fairly constant for small displacements (i.e., $x << a$) and that this value depends on the ratio, b/a^2. From this expression, it is observed that the frequency of the surface is inversely proportional to the square of semi-major axis and that an increase in its value results in a sharp decrease in the isolator frequency. Hence, in order to get the desired variation in the isolator frequency, the semi-major axis of the ellipse, a, is taken as a linear function of the sliding displacement x and is expressed as a variable in getting the geometry of VFPI. The semi-major axis can thus be expressed as

$$a = x + d \tag{7}$$

where d is a constant. On substituting Equation (7) in Equation (4), the expression for the geometry of the sliding surface of VFPI becomes

$$y = b\left[1 - \frac{\sqrt{d^2 + 2dx\,\mathrm{sgn}(x)}}{d + x\,\mathrm{sgn}(x)}\right] \tag{8}$$

where $\mathrm{sgn}(x)$ is the signum function introduced for maintaining the symmetry of sliding surface about the central vertical axis. This function assumes a value of +1 for the positive sliding displacements and −1 for the negative sliding displacements. It is observed from Equation (8) that the upper bound of vertical displacements is equal to b and that this occurs only at infinitely large horizontal displacements. The slope at any point on this sliding surface is given as

$$\frac{\mathrm{d}y}{\mathrm{d}x} = \frac{bd}{\left(d + x\,\mathrm{sgn}(x)\right)^2 \sqrt{d^2 + 2d\ \mathrm{sgn}(x)}}\,x \tag{9}$$

To simplify the notations, a non-dimensional parameter $r = x\,\mathrm{sgn}(x)/d$ is used. On substituting r and the initial frequency squared $\omega_I^2 = gb/d^2$ in Equation (9) and on combining with Equations (1) and (2), the square of the isolator frequency at any sliding displacement can be expressed as

$$\omega_b^2(x) = \frac{\omega_I^2}{(1+r)^2\sqrt{1+2r}} \tag{10}$$

In the above equations, the parameters b and d completely define the isolator characteristics. It can also be observed that the ratio, b/d^2, governs the initial frequency of the isolator. Similarly, the value of $1/d$ determines the rate of variation of the isolator frequency. Let this factor be defined as the frequency variation factor (FVF). It is also seen from Equation (10) that the rate of decrease in the isolator frequency is directly proportional to FVF for a given initial frequency. The variation in the oscillation frequency of a typical VFPI with respect to sliding displacement is shown in Figure 2(a). For the purpose of comparison, the oscillation frequency of FPS with the same initial frequency is also shown and is found to be almost constant. From this plot, it is seen that the oscillation frequency of VFPI sharply decreases with the increasing sliding displacement and asymptotically approaches zero. The force-deformation hysteresis curves obtained from Equation (3), for a typical FPS and VFPI, are shown in Figure 2(b). In this plot, the isolator force (i.e., restoring force plus frictional force) is normalized with respect to mg and both constant and discretely variable coefficients of friction are considered. It can be observed that the isolator force in VFPI first increases to reach its maximum value and later decreases slowly so as to asymptotically approach the frictional force at large sliding displacements for a constant coefficient of friction. This is an important property of VFPI, which limits the force transmitted to the structure. Beyond the peak restoring force, the VFPI does not lose the restoring capability since a small amount of restoring force is always available. It is also observed that for very small displacements, the variation in restoring

force is approximately linear. In the FPS, on the other hand, the restoring force always increases linearly with the sliding displacement. From this, it can be concluded that the behaviour of VFPI is similar to that of FPS for small displacements and similar to that of PF for large displacements without a significant loss of restoring capability. In the case of a variable coefficient of friction, the isolator force suddenly changes at a point where the coefficient of friction undergoes a change in its value, while the rest of the variation remains unchanged. This will change the energy dissipation characteristics of the isolator which may help in controlling the sliding displacements.

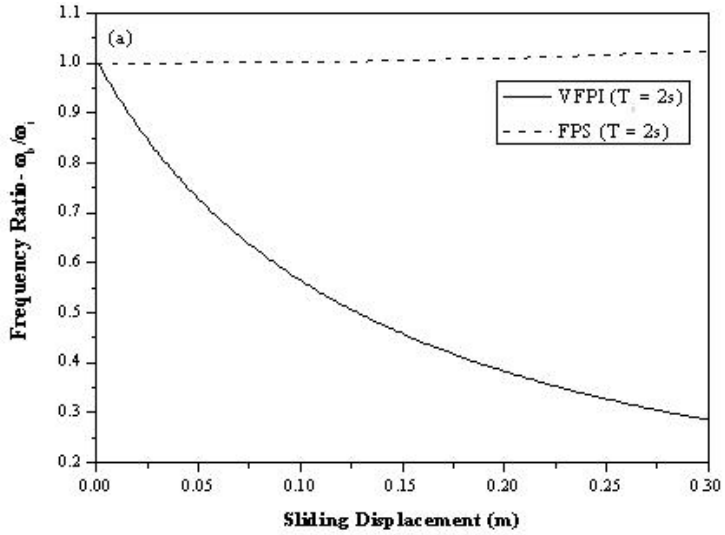

(a)

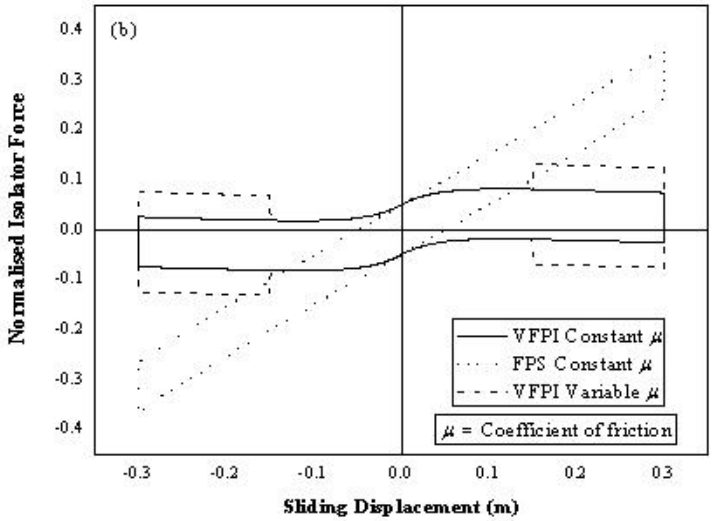

(b)

Fig. 2 Comparison of variations of (a) frequency ratio and (b) normalized isolator force with sliding displacement for VFPI and FPS (with $\mu = 0.05$, $\mu_1 = 0.05$ and $\mu_2 = 0.1$)

The geometries of the sliding surfaces of VFPI and FPS are shown in Figure 3. From this figure, it can be easily observed that a VFPI is flatter than a FPS, which results in smaller vertical displacements for similar sliding displacements in the structure and hence may lead to smaller overturning moments.

MATHEMATICAL FORMULATION

Consider a single-storey shear structure isolated by a sliding type isolator (i.e., a two-DOF system when isolated) when it is subjected to the horizontal ground excitation $\ddot{x}_g$ (see Figure 4). The forces acting on the isolator, when sliding is in the positive x-direction, are same as those shown in Figure 1.

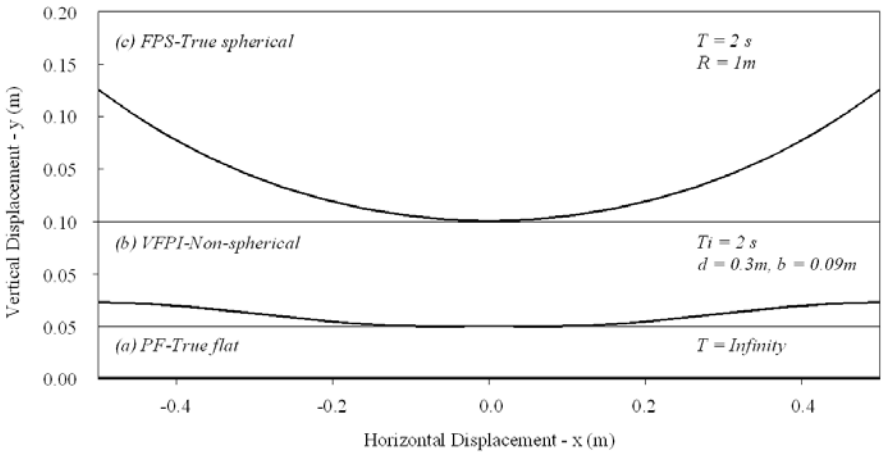

Fig. 3 Geometries of sliding surfaces of PF, VFPI and FPS isolators

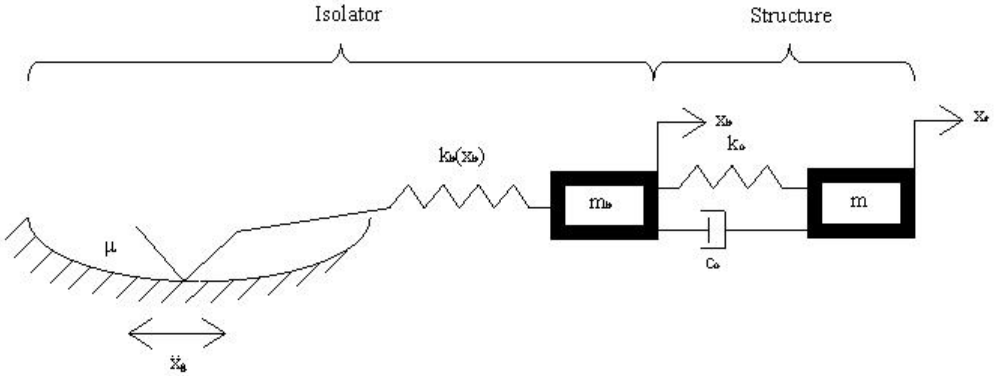

Fig. 4 Analytical model of single-storey structure isolated by curved sliding surface

1. Equations of Motion

The motion of structure can be in either of the two phases: non-sliding phase and sliding phase. In the non-sliding phase, the structure behaves like a conventional fixed-base structure, since there is no relative motion at the isolator level. When the frictional force at the sliding surface is overcome, there is a relative motion at the sliding surface and the structure enters the sliding phase. The total motion consists of a series of alternating non-sliding and sliding phases in succession.

2. Non-sliding Phase

In the non-sliding phase, the structure behaves as a fixed-base structure. There is no relative motion between the ground and base mass, since the static frictional resistance is greater than the horizontal force acting on the structure. The equations of motion in this phase are

$$\ddot{x}_r + 2\xi_o\omega_o\dot{x}_r + \omega_o^2 x_r = -\ddot{x}_g \tag{11}$$

and

$$x_b = \text{constant};\ \dot{x}_b = \ddot{x}_b = 0 \tag{12}$$

where x_r is the relative displacement of the top mass with respect to the base mass, x_b is the displacement of the base mass m_b relative to the ground, and x_g is the ground displacement. Further, an overdot indicates a derivative with respect to time, and $\omega_o = \sqrt{k_o/m}$ and $\xi_o = c_o/2\sqrt{k_o m}$ are the frequency and damping ratio, respectively, of the fixed-base SDOF structure. Before the application of ground motion, the structure is at rest; as a result, the motion of structure always starts in the non-sliding phase. The structure is classically damped in this phase and hence the equation of motion can be readily solved by the usual modal analysis procedures (Clough and Penzien, 1993).

3. Initiation of Sliding Phase

When the structure is subjected to a base excitation, it will remain in the non-sliding phase unless the frictional resistance at the sliding surface is overcome. This means that the absolute value of the sum of the total inertia force and restoring force should be greater than or equal to the absolute value of the frictional force acting along the sliding surface. The frictional force depends on the coefficient of friction at the location at a given instant. The plan of a typical isolator with two discrete values of the coefficient of friction considered in this study is shown in Figure 5. The coefficient of friction, μ_1, is assumed to be less than μ_2 in this study. Therefore, the condition for the beginning of the sliding phase can be written as

$$\left|\left[m\left(\ddot{x}_r+\ddot{x}_g\right)+m_b\ddot{x}_g\right]\cos\theta+\left(m+m_b\right)g\sin\theta\right|\geq\mu\left(m+m_b\right)g\cos\theta \tag{13}$$

where θ is the angle of tangent at the point of contact with horizontal and μ (= μ_1 or μ_2) is the coefficient of friction at the respective isolator positions. Now, on dividing Equation (13) by $\cos\theta$ and substituting $\mathrm{d}y/\mathrm{d}x_b$ for $\tan\theta$, the condition for sliding can be simplified as

$$\left|\left[m\left(\ddot{x}_r+\ddot{x}_g\right)+m_b\ddot{x}_g\right]+\left(m+m_b\right)g\frac{\mathrm{d}y}{\mathrm{d}x_b}\right|\geq\mu\left(m+m_b\right)g\;;\;\mu=\mu_1\text{ or }\mu_2 \tag{14}$$

Here, $\left(m+m_b\right)g\,\mathrm{d}y/\mathrm{d}x_b$ is the restoring force (see Equation (1)). If this is expressed as a product of the spring stiffness and sliding displacement, the spring force is given by (see Equation (3))

$$f_R=\left(m+m_b\right)\omega_b^2\left(x_b\right)x_b \tag{15}$$

where $\omega_b\left(x_b\right)$ is the isolator frequency at the instant for the sliding displacement x_b. On dividing Equation (14) by the total mass and on defining the mass ratio as

$$\alpha=\frac{m}{m+m_b} \tag{16}$$

the condition for the initiation of the sliding phase can be simply expressed as

$$\left|\alpha\ddot{x}_r+\ddot{x}_g+\omega_b^2\left(x_b\right)x_b\right|\geq\mu g\;;\;\mu=\mu_1\text{ or }\mu_2 \tag{17}$$

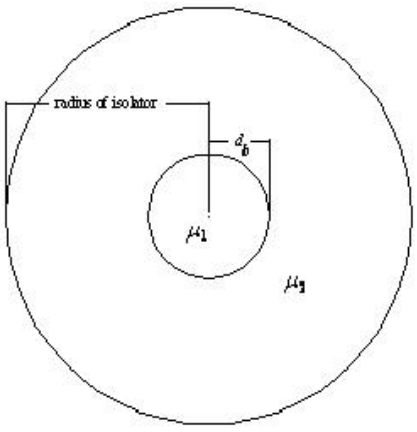

Fig. 5 Plan of typical isolator with variable coefficient of friction

4. Sliding Phase

Once the inequality (see Equation (14)) is satisfied, the static frictional force is overcome, the structure enters the sliding phase, and the degree of freedom (DOF) corresponding to the base mass also experiences motion. During this phase, the structure behaves like a two-degree-of-freedom structure. The equations of motion for the top and bottom masses are respectively given by

$$\ddot{x}_r + 2\xi_o\omega_o\dot{x}_r + \omega_o^2 x_r = -\ddot{x}_b - \ddot{x}_g \tag{18}$$

and

$$\alpha\ddot{x}_r + \ddot{x}_b + \omega_b^2\left(x_b\right)x_b = -\ddot{x}_g - \mu g\,\mathrm{sgn}\left(\dot{x}_b\right);\ \mu = \mu_1 \text{ or } \mu_2 \tag{19}$$

5. End of Sliding Phase

The sliding phase ends when the sliding velocity of the base mass becomes equal to zero, i.e.,

$$\dot{x}_b = 0 \tag{20}$$

As soon as this condition is satisfied, Equations (11) and (12) corresponding to the non-sliding phase need to be evaluated to further check the validity of the inequality in Equation (17). This decides whether the structure continues in the sliding phase after a momentary stop or enters the non-sliding phase.

6. Direction of Sliding

Once the inequality (see Equation (17)) is satisfied, the structure starts sliding in a direction opposite to the direction of the sum of the total inertia force and restoring force at the isolator level. Thus, the direction of sliding can be decided based on the signum function as defined below:

$$\mathrm{sgn}\left(\dot{x}_b\right) = -\frac{\alpha\dot{x}_r + \ddot{x}_g + \omega_b^2\left(x_b\right)}{\left|\alpha\dot{x}_r + \ddot{x}_g + \omega_b^2\left(x_b\right)\right|} \tag{21}$$

The signum function remains unchanged in a particular sliding phase until the sliding velocity of the base mass becomes equal to zero. Once the sliding velocity is zero, the structure may enter the non-sliding phase, reverse its direction of sliding, or have a momentary stop and then continue in the same direction. To determine the correct state, the solution process needs to continue while using the equations of non-sliding phase wherein the sliding acceleration is forced to be zero and the validity of the inequality (see Equation (17)) is checked. If this inequality is satisfied at the same instant of time when the sliding velocity is zero, Equation (21) decides the further direction of sliding.

RESPONSE OF AN EXAMPLE SYSTEM

The effectiveness of VFPI with a variable coefficient of friction to reduce the response of an example single-storey structure subjected to the near-fault earthquake excitations is presented in this section. The example structure, under the fixed-base condition, is represented as an SDOF system, with the values of spring stiffness and lumped mass taken such that the period of the structure is 0.5 s. The masses of the structure and base are taken equal, such that the mass ratio α becomes 0.5.

Narasimhan and Nagarajaiah (2006) proposed a variable-friction system to adjust the level of friction in the base-isolated structures. Panchal and Jangid (2008) proposed a sliding surface by varying the friction coefficient along the sliding surface in the form of the curve of FPS and called the isolator as VFPS. In this case, the value of the coefficient of friction changes from a minimum of 0.025 to a maximum of 0.15 and then again reduces and approaches ~0.015. Krishnamoorthy (2010) proposed a variable frequency and variable friction pendulum isolator (VFFPI). Here, the value of the coefficient of friction changes from a minimum of 0.08 to a maximum of 0.1 in between the distance of 0.0 to 0.18 m from the centre of the sliding surface. These studies show that a sliding isolator with either a varying radius of curvature or a varying friction coefficient may be used as an effective isolator for isolating the structure. Most of these studies have focussed on the effectiveness of the isolator in reducing accelerations under different excitations. However, all of these isolators are likely to be of limited effectiveness under the near-fault ground motions due to very high sliding displacements. Further, it may be practically difficult to achieve a sliding surface with a continuously variable coefficient of friction of desired variation. Hence, in the present study, the performance of VFPI with two discrete values of the coefficient of friction, i.e., the initial coefficient of friction, μ_1, and the final coefficient of friction, μ_2, under the near-fault ground motions is evaluated.

The behaviour of VFPI is studied through a time-history analysis for ten near-fault ground motion records. The details of the ground-motion records used in the study are presented in Table 1. These ground-motion records are derived from the actually recorded motions. The ground motions chosen cover

a wide variety of near-fault ground motions having different peak ground acceleration (PGA) values, frequency compositions and durations. For a given coefficient of friction, the main parameters of VFPI affecting the response are (i) initial time period and (ii) frequency variation factor (FVF). For the present analysis, FVF is varied from 1.0 per m to 10.0 per m for a VFPI with two values of initial time period, 1 and 2 s. In order to investigate the effectiveness of VFPI, the responses are compared with those of the structure isolated by using a FPS with the isolator period equal to 2.0 s, which is a practical value for such a system.

Table 1: Details of Ground-Motion Records Used in This Study

S. No.	Name of Earthquake	Designation	Magnitude	Distance of Source (km)	PGA (*g*)	Duration (s)
1	1978 Tabas	NFR-01	7.4	1.2	0.900	50
2	1989 Loma Prieta	NFR-02	7.0	3.5	0.718	25
3	1989 Loma Prieta	NFR-03	7.0	6.3	0.686	40
4	1992 Cape Mendocino	NFR-04	7.1	8.5	0.638	60
5	1992 Erzincan	NFR-05	6.7	2.0	0.432	21
6	1992 Landers	NFR-06	7.3	1.1	0.713	50
7	1994 Nothridge	NFR-07	6.7	7.5	0.890	15
8	1994 Nothridge	NFR-08	6.7	6.4	0.732	60
9	1995 Kobe	NFR-09	6.9	3.4	1.088	60
10	1995 Kobe	NFR-10	6.9	4.3	0.786	40

In order to study the effect of variable coefficient of friction on the behaviour of a VFPI-isolated structure, two values of the coefficient of friction considered are $\mu_1 = 0.05$ and $\mu_2 = 0.1$. The VFPIs with these two constant coefficients of friction are first analyzed separately and then they are combined in the same isolator, the latter case being referred to as the case of variable coefficient of friction. In this case the initial coefficient of friction, μ_1, refers to the coefficient of friction up to a pre-defined distance d_b from the centre of the isolator, and the coefficient of friction beyond this distance is referred to as the final coefficient of friction, μ_2. The values $\mu_1 = 0.05$ and $\mu_2 = 0.1$ considered in this study should enable a larger energy dissipation for a larger sliding displacement, which may help to control the sliding displacements. For the change of coefficient of friction, three positions are considered from the centre of the isolator: $d_b = 0.1$, 0.3 and 0.5 m. The structural damping is assumed as 5% of critical.

1. Time-History Response

The response quantities are evaluated by the solution of the equations of motion as discussed in the preceding sections. The main response quantities of interest are the absolute acceleration of the top storey and the sliding displacement of the isolator. To show the effectiveness of VFPI with respect to FPS, typical time-history graphs for NFR-01 (i.e., the normal component of the 1978 Tabas earthquake motion) are shown in Figures 6 and 7. Figure 6 shows the acceleration time histories for VFPI and FPS with the constant coefficient of friction of 0.05. As expected, it is seen that the accelerations are substantially reduced in the case of VFPI as compared to FPS.

It is expected that varying the coefficient of friction along the sliding surface will lead to a decrease in the sliding displacement. This is usually a matter of concern for the VFPIs, especially under the near-field ground motions. To show the effectiveness of the variable coefficient of friction, typical time-history graphs of sliding displacement under NFR-01 are shown in Figure 7. This figure shows the time-histories of sliding displacement for the cases of constant coefficient of friction and variable coefficient of friction under the three different values of d_b. It is seen that the sliding displacements are effectively controlled in the case of variable coefficient of friction and that this case is more effective for the lesser values of

d_b. This implies that it is possible to control the sliding displacements by using a variable coefficient of friction under the near-field ground motions without any significant increase in the accelerations.

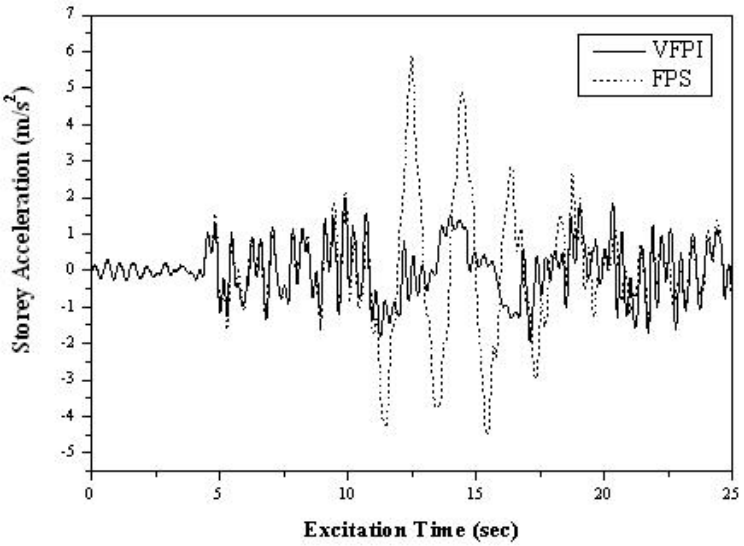

Fig. 6 Comparison of time-history curves of storey acceleration for VFPI and FPS with constant coefficient of friction (for NFR-01, FVF = 2 and $\mu = 0.05$)

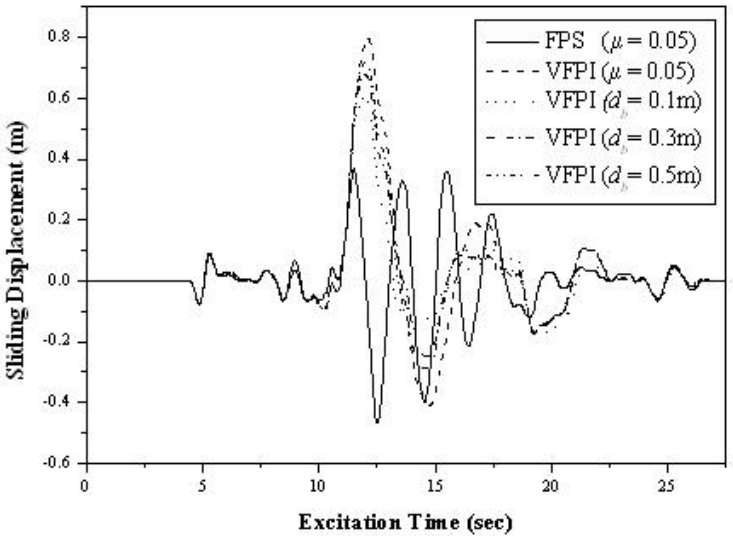

Fig. 7 Comparison of time-history curves of sliding displacement for VFPI and FPS with constant and variable coefficients of friction (for NFR-01, FVF = 2, $\mu = 0.05$, $\mu_1 = 0.05$ and $\mu_2 = 0.1$)

To further ascertain the effectiveness of variable coefficient of friction in reducing the sliding displacements, a comparison of the force-deformation histories for constant and variable coefficients of friction in the VFPI of T_i = 2 s is presented in Figure 8 for the case of NFR-01, FVF = 2 and d_b = 0.1 m. From this figure, it is clear that sliding displacements are controlled in the case of variable coefficient of friction due to higher energy dissipation in this case, since the area under the force-deformation graph increases due to the increased coefficient of friction at the predefined point.

2. Effect of Variable Coefficient of Friction

Under the near-fault excitations, a FPS may be able to control the sliding displacements, but it may also lead to very high levels of structural accelerations due to the long-period pulse-type components in the excitation. On the other hand, a VFPI can control the accelerations but at the cost of high sliding

displacements. Hence, a VFPI with variable coefficient of friction is likely to control both accelerations and sliding displacements. Varying the coefficient of friction may not help in the case of FPS as the displacements are already controlled with a constant coefficient of friction and accelerations are bound to be high in any case due to the constant time period of FPS. In order to present the responses with effective comparison and comprehension, the maximum response quantities of the structures isolated with a VFPI are normalized with respect to the corresponding response quantity, with the FPS having a constant time period of 2.0 s and the corresponding value of the coefficient of friction. For example, the maximum response values with the VFPI of μ = 0.05 are normalized with respect to the maximum response value with the FPS of μ = 0.05, and the maximum response values with the VFPI of μ = 0.1 are normalized with respect to the maximum response value with the FPS of μ = 0.1. In the case of variable coefficient of friction, the response quantities are normalized with the FPS having a constant coefficient of friction of 0.05, since varying the coefficient of friction in the case of FPS will not add to any advantage in the performance. This means that the maximum response values with a VFPI of variable coefficient of friction are normalized with respect to the maximum response value with the FPS of μ = 0.05. Thus, the isolation is more effective when the normalized accelerations are less than unity (i.e., less than the corresponding response with the FPS) and the normalized sliding displacements are marginally greater than unity (which is the displacement control equivalent to the FPS).

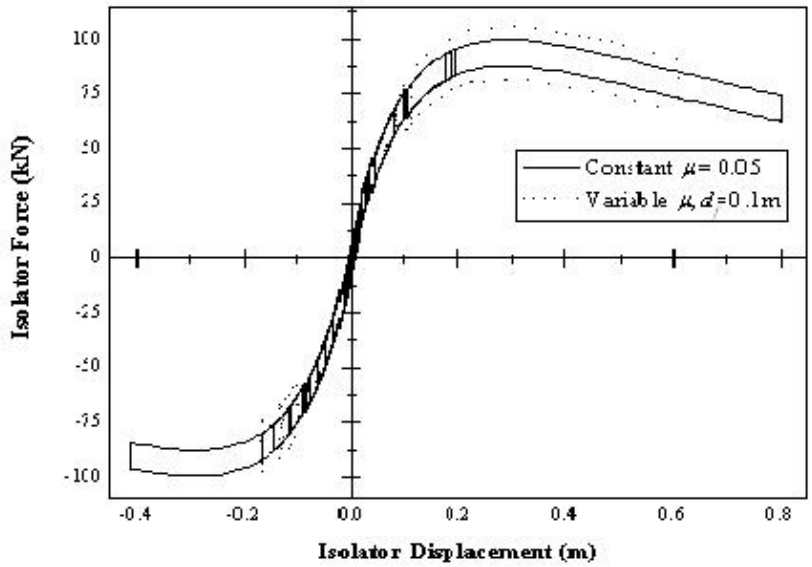

Fig. 8 Comparison of force-deformation histories of VFPI for constant and variable coefficients of friction (for NFR-01, FVF = 2, $\mu = 0.05$, $\mu_1 = 0.05$, $\mu_2 = 0.1$ and $d_b = 0.1$ m)

For different cases under consideration, time-history analyses are carried out for all the ten near-fault ground motions described in Table 1. Since these ground motions cover a wide variety of near-fault ground motions, the average of the maximum responses under the ten ground motions is considered for discussion. This is normalized by the average response of the corresponding FPS-isolated structures as explained earlier. The averages of maximum storey acceleration and sliding displacement responses with the FPS, using which the averages of maximum responses with the VFPI are normalized, are given in Table 2 for μ = 0.05 and 0.1. The normalized storey accelerations with the VFPIs for two constant and three variable coefficients of friction cases are compared in Figures 9 and 10 respectively for T_i = 1 and 2 s. Similarly, the normalized average sliding displacements with the VFPIs for two constant and three variable coefficients of friction cases are compared in Figures 11 and 12 respectively for T_i = 1 and 2 s.

From Figures 9 and 10, as expected, it is observed that the accelerations in the VFPI-isolated system are substantially reduced when compared to those in the FPS-isolated system, in all the cases. When the initial time period of VFPI is 1.0 s, it is observed that the accelerations sharply decrease with FVF (because of the sharp decrease in the restoring force), whereas there is no significant decrease in the accelerations with FVF in the case of VFPI with the initial time period of 2.0 s. Further, as expected, the

accelerations under a lower coefficient of friction of 0.05 are substantially lower than those with a higher coefficient of friction of 0.1. The same observation also holds true in the cases of variable coefficient of friction, and the accelerations in all such cases (with different values of d_b) fall in between the accelerations for the two cases of constant coefficient of friction. However, those are closer to the lower bound of accelerations (i.e., for the case of the coefficient of friction of 0.05), which shows the effectiveness of a variable coefficient of friction in acceleration reduction.

Table 2: Average Peak Response Values for FPS-Isolated Structure with T = 2 s

S. No.	Description of Response	Unit	Peak Response Values for Coefficient of Friction	
			0.05	**0.1**
1	Storey acceleration	m/s^2	12.915	8.140
2	Sliding displacement	m	0.614	0.490

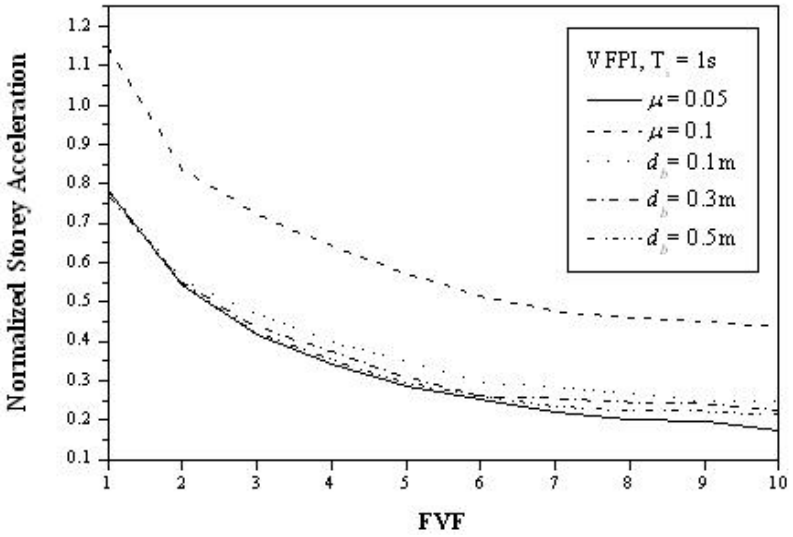

Fig. 9 Comparison of storey accelerations with different cases of VFPIs (of T_i = 1 s) as normalized with respect to peak values with FPS as in Table 2

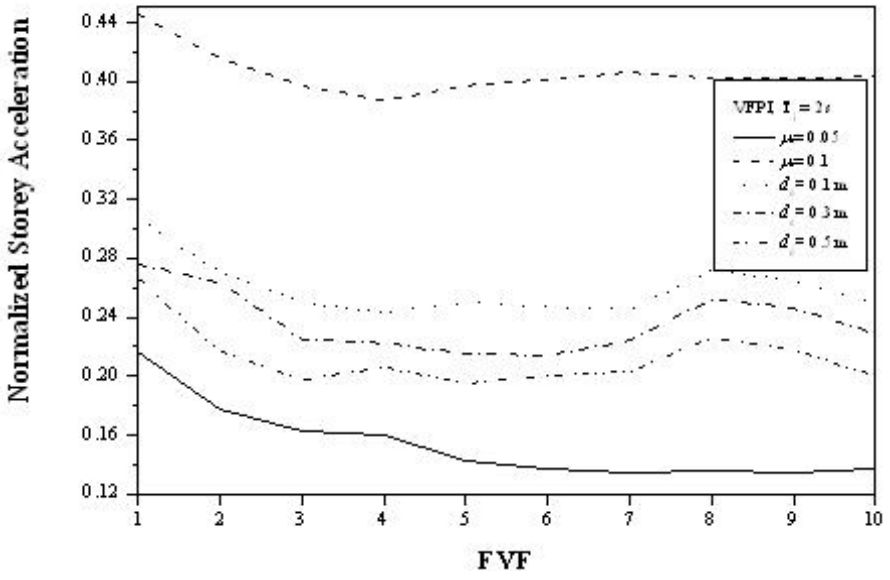

Fig. 10 Comparison of storey accelerations with different cases of VFPIs (of T_i = 2 s) as normalized with respect to peak values with FPS as in Table 2

From Figures 11 and 12, it is observed that the normalized sliding displacements increase with an increase in FVF in all the cases, since the increase in FVF leads to a reduction in the restoring force. As expected, the displacements for the lower coefficient of friction are higher than those for the higher coefficient of friction. It is interesting to note that the sliding displacements in some cases of variable coefficient of friction (see, for example, the results for d_b = 0.1 m) are lower than those in both the cases of constant coefficient of friction. It is also seen that sliding displacements are significantly lower for a FVF of 4–6 for the VFPI with the initial time period of 1.0 s and for a FVF of 1 to 3 for the VFPI with the initial time period of 2.0 s. It can be further confirmed that for this range of FVF, the accelerations are also significantly lower (around 20% to 30% of those in the case of FPS). Thus, it can be concluded that by varying the coefficient of friction at a suitable location on the isolator surface and by selecting suitable FVF and initial time period, it is possible to control both accelerations and sliding displacements.

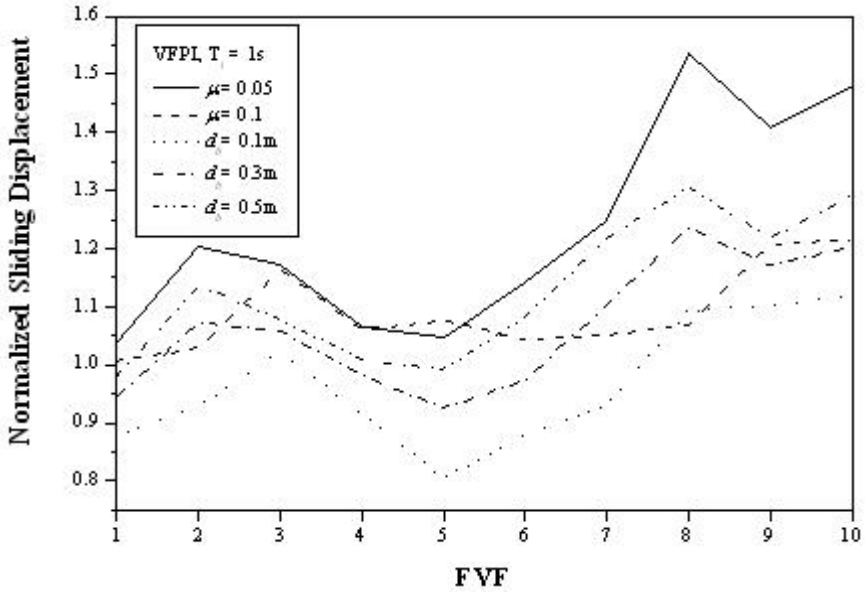

Fig. 11 Comparison of sliding displacements with different cases of VFPIs (of T_i = 1 s) as normalized with respect to peak values with FPS as in Table 2

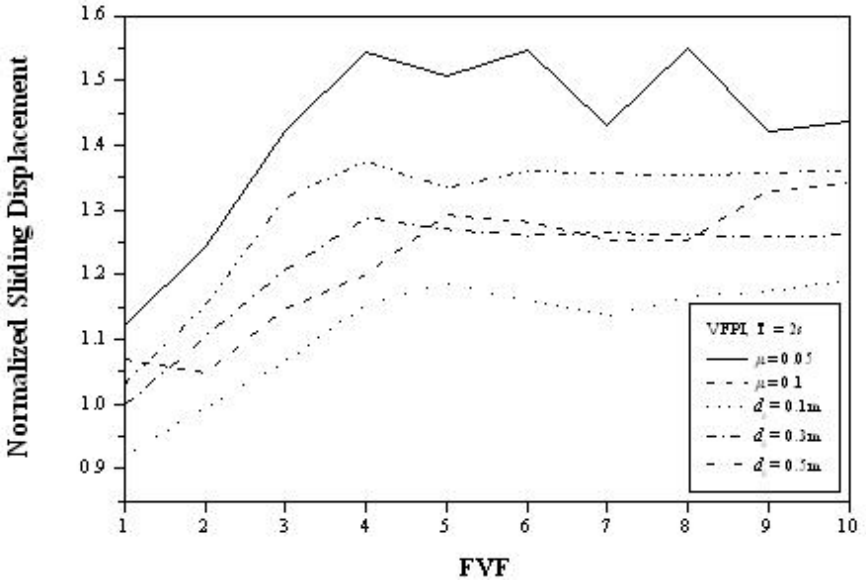

Fig. 12 Comparison of sliding displacements with different cases of VFPIs (of T_i = 2 s) as normalized with respect to peak values with FPS as in Table 2

CONCLUSIONS

The effectiveness of a recently developed isolation system, the variable frequency pendulum isolator (VFPI), for the vibration control of a single-storey structure subjected to the near-fault ground motions has been investigated in this paper. For the effectiveness of a VFPI in controlling both accelerations and sliding displacements under the near-field ground motions, a variable coefficient of friction for the sliding surface has been proposed in this paper. Based on the investigations, the following conclusions can be drawn:

1. A VFPI has a wide choice of parameters that can be chosen to suit the design requirements.
2. A VFPI is very effective for acceleration reduction under the action of near-fault ground motions, with a corresponding increase in the sliding displacements.
3. It is possible to control both accelerations and sliding displacements by using a variable coefficient of friction and by carefully choosing the VFPI parameters.

REFERENCES

1. Buckle, I.G. and Mayes, R.L. (1990). “Seismic Isolation: History, Application, and Performance—A World View”, Earthquake Spectra, Vol. 6, No. 2, pp. 161–201.
2. Clough, R.W. and Penzien, J. (1993). “Dynamics of Structures”, McGraw-Hill, New York, U.S.A.
3. Kelly, J.M. (1993). “State-of-the-Art and State-of-the-Practice in Base Isolation”, Proceedings of ATC-17-1 Seminar on Seismic Isolation, Passive Energy Dissipation, and Active Control, San Francisco, U.S.A., Vol. 1, pp. 9–28.
4. Krishnamoorthy, A. (2010). “Seismic Isolation of Bridges Using Variable Frequency and Variable Friction Pendulum Isolator System”, Structural Engineering International, Vol. 20, No. 2, pp. 178–184.
5. Lu, L.-Y., Wang, J. and Hsu, C.-C. (2006). “Sliding Isolation Using Variable Frequency Bearings for Near-Fault Ground Motions”, Proceedings of the 4th International Conference on Earthquake Engineering, Taipei, Taiwan, Paper No. 164 (on CD).
6. Malu, G. and Murnal, P. (2010). “Behavior of Structure with VFPI during Near-Field Ground Motion”, Proceedings of International Conference on Innovative World of Structural Engineering (ICIWSE-2010), Aurangabad, Vol. I, pp. 166–174.
7. Mokha, A., Constantinou, M. and Reinhorn, A. (1990). “Teflon Bearings in Base Isolation. I: Testing”, Journal of Structural Engineering, ASCE, Vol. 116, No. 2, pp. 438–454.
8. Mostaghel, N., Hejazi, M. and Tanbakuchi, J. (1983). “Response of Sliding Structures to Harmonic Support Motion”, Earthquake Engineering & Structural Dynamics, Vol. 11, No. 3, pp. 355–366.
9. Murnal, P. and Malu, G.M. (2007). “Selection of VFPI Parameters for Isolation Effectiveness during Near-Field Ground Motion”, Proceedings of the 8th Pacific Conference on Earthquake Engineering, Singapore, Paper No. 105 (on CD).
10. Naeim, F. and Kelly, J.M. (1999). “Design of Seismic Isolated Structures: From Theory to Practice”, John Wiley, New York, U.S.A.
11. Narasimhan, S. and Nagarajaiah, S. (2006). “Smart Base Isolated Buildings with Variable Friction Systems: H_∞ Controller and SAIVF Device”, Earthquake Engineering & Structural Dynamics, Vol. 35, No. 8, pp. 921–942.
12. Panchal, V.R. and Jangid, R.S. (2008). “Variable Friction Pendulum System for Seismic Isolation of Liquid Storage Tanks”, Nuclear Engineering and Design, Vol. 238, No. 6, pp. 1304–1315.
13. Pranesh, M. (2000). “VFPI: An Innovative Device for Aseismic Design”, Ph.D. Thesis, Indian Institute of Technology Bombay, Mumbai.
14. Pranesh, M. and Sinha, R. (1998). “Vibration Control of Primary-Secondary Systems Using Variable Frequency Pendulum Isolator”, Proceedings of the Eleventh Symposium on Earthquake Engineering, Roorkee, Vol. II, pp. 697–704.
15. Shustov, V. (1992). “Base Isolation: Fresh Insight”, Proceedings of the Tenth World Conference on Earthquake Engineering, Madrid, Spain, Vol. 4, pp. 1983–1986.

16. Sinha, R. and Pranesh, M. (1998). "FPS Isolator for Structural Vibration Control", Proceedings of International Conference on Theoretical, Applied, Computational and Experimental Mechanics (ICTACEM98), Kharagpur (on CD).
17. Somerville, P. (1997). "Engineering Characteristics of Near Fault Ground Motion", Proceedings of SMIP97 Seminar on Utilization of Strong-Motion Data, Los Angeles, U.S.A., pp. 9–28.
18. Somerville, P.G. (2005). "Engineering Characterization of Near Fault Ground Motions", Proceedings of 2005 New Zealand Society for Earthquake Engineering Conference, Taupo, New Zealand, Paper No. 1 (on CD).
19. Tsai, C.S. (1997). "Finite Element Formulations for Friction Pendulum Seismic Isolation Bearings", International Journal for Numerical Methods in Engineering, Vol. 40, No. 1, pp. 29–49.
20. Tsopelas, P., Constantinou, M.C., Kim, Y.S. and Okamoto, S. (1996). "Experimental Study of FPS System in Bridge Seismic Isolation", Earthquake Engineering & Structural Dynamics, Vol. 25, No. 1, pp. 65–78.
21. Wang, Y.-P., Chung, L.-L. and Liao, W.-H. (1998). "Seismic Response Analysis of Bridges Isolated with Friction Pendulum Bearings", Earthquake Engineering & Structural Dynamics, Vol. 27, No. 10, pp. 1069–1093.
22. Zayas, V.A., Low, S.S. and Mahin, S.A. (1987). "The FPS Earthquake Resisting System: Experimental Report", Report UCB/EERC-87/01, University of California, Berkeley, U.S.A.
23. Zayas, V.A., Low, S.S. and Mahin, S.A. (1990). "A Simple Pendulum Technique for Achieving Seismic Isolation", Earthquake Spectra, Vol. 6, No. 2, pp. 317–333.